

## **Numerical analysis of sapphire crystal growth by the Kyropoulos technique**

S.E. Demina<sup>1</sup>, E.N. Bystrova<sup>1</sup>, M.A. Lukanina<sup>1</sup>, V.M.Mamedov<sup>2</sup>, V.S. Yuferev<sup>2</sup>, E.V. Eskov<sup>3</sup>,  
M.V. Nikolenko<sup>3</sup>, V.S. Postolov<sup>3</sup>, V.V. Kalaev<sup>\*4</sup>

<sup>1</sup> *Soft-Impact, Ltd, P.O. Box 83, 194156, St. Petersburg, Russia*

<sup>2</sup> *Ioffe Physico-Technical Institute, 194021 St. Petersburg, Russia*

<sup>3</sup> *Monocrystal Inc., 355035, Stavropol, Russia*

<sup>4</sup> *Semiconductor Technology Research GmbH, Eltersdorferstr. 22, 91058 Erlangen, Germany*

### **Abstract**

A numerical model has been suggested to analyze processes occurring during sapphire crystal growth by the Kyropoulos technique. The model accounts for the radiative heat exchange in the crystal and melt convection together with the crystallization front formation. The theoretical predictions agree well with available experimental data.

**PACS:** 81.10.Aj, 81.10.Fq, 02.60.Cb

**Keywords:** Numerical simulation; Sapphire; Kyropoulos; Crystal

### **1. Introduction**

Lately, there has been much interest in growing sapphire crystals of large size and weight to increase the effectiveness of sapphire growth technologies. For example, Monocrystal Inc. in Stavropol (Russia) has developed an exclusive Kyropoulos method allowing the production of sapphire boules with a diameter up to 300 mm and 65 kg weight (see Fig. 1).

A better crystal quality and yield ratio can be achieved by improving the hot zone of the Kyropoulos furnace, which can be done with an efficient support of numerical simulation. In the present work, Kyropoulos crystal growth is considered within a 2D axisymmetric approach accounting for the heat transfer in the whole system as well as radiative heat exchange in the crystal, melt convection, and crystallization front formation in the crystallization zone. This approach has been tested on a simplified reactor design, a so called model reactor, as well as on several modifications of an industrial growth setup. The computations show a significant effect of melt convection on the crystallization front, and the temperature gradients in the crystal and the melt. Ways of governing the melt flow are discussed as a tool to improve crystal quality, which can be predicted from the calculations of crystal thermal stresses.

### **2. Model**

The approach we suggest requires a pre-computation of the global heat transfer in the whole system. Then, the heat exchange is modeled only in the crystallization zone including the crystal, the melt, the crucible, and the gas region around the crystal. The computation involves the turbulence flow of the sapphire melt, the laminar gas flow, and the radiative heat exchange in the semi-transparent crystal.

To compute the global heat transfer, we used the axisymmetric model suggested in [1], which accounts for heat transfer via conduction and radiation between the solid surfaces. The heat transfer and melt convection in the crystallization zone were computed using the approach described in [2]. In this approach, the heat fluxes obtained from the global heat transfer computation were used as the thermal boundary conditions at the external boundaries of the domain. To account for the crystal semitransparency, we used an approach developed in [3] in terms of the discrete transfer method for solving problems of the radiation transfer in axisymmetric areas of complex geometry with specular Fresnel's boundaries. The specular reflectivity used in our computations for unpolarized radiation and a dielectric medium is determined by Fresnel's formula.

The computations were made using the CGSim package [www.semitech.us](http://www.semitech.us).

---

\*Corresponding author. Tel.: +49 172 838 7236; fax: +49 913 197 2398  
E-mail address: [Vladimir.Kalaev@strgmbh.de](mailto:Vladimir.Kalaev@strgmbh.de)

### 3. Results

#### 3.1. Analysis of global heat transfer in the model reactor

The simplified model reactor was used to compute the global heat transfer with a detailed analysis of the heat flux distribution. The crystal is assumed to be opaque and the melt to be solid with the effective thermal conductivity:  $\kappa_c = 5.8 \text{ W/mK}$  and  $\kappa_m = 10 \text{ W/mK}$ , respectively. Fig. 2 shows the heat flux vector (a) and the temperature distributions (b) in the reactor. The maximal temperature in the reactor is 2390 K. The main heat flux is distributed in the following way: 20% down, 27% up, and 53% sideways, which agrees well enough with the temperature drop measurements in the cold system of the industrial furnace. One can see that the flux intensity increases away from the heater towards the screens. The flux in the crucible goes down to the support and up to the screens. In the melt, the flux is fairly uniform while it increases towards the seed in the crystal. The distributions in Fig. 2 illustrate the heat flux along the side wall (c) and the bottom (d) of the crucible. The sign “-“ means that the heat goes to the surface heating it; the sign “+” means that the flux goes away from the surface which gets cold. The heat power through these boundaries is about 5200 and 417 W, respectively.

#### 3.2. Computation of heat transfer and hydrodynamics in the crystallization zone

For the two modifications of the hot zone in the industrial furnace, we computed the global heat transfer, the heat transfer in the hot zone with radiative heat exchange in the crystal and melt convection together with the crystallization front formation. The focus was on the effect of the reactor design on the temperature distribution in the whole setup, the crystallization front shape, and the temperature gradient changes in the crystal and the melt. Special attention was given to the analysis of the flow pattern in the crystallization zone. In the global heat transfer we used the effective thermal conductivity  $\kappa_c = 300 \text{ W/mK}$  and  $\kappa_m = 10 \text{ W/mK}$  adjusted such that the temperature differences in the crystal and the melt were close to those in the computation with convection. The optical properties used for the account of the sapphire semitransparency are i) the transparent band is 0.5-4.5 micron with the absorption coefficient  $19.26 \text{ m}^{-1}$ , ii) the refractive index is 1.78, and iii) the scattering coefficient is 0.

Fig. 3 demonstrates the temperature distribution and the flow pattern in the hot zone and the temperature gradient in the crystal for two modifications: Modification 1 and Modification 2. The computations show that the melt convection affects much the crystallization front shape and the temperature gradient in the crystal and the melt. In Modification 1, the flow melt has a two-vortex structure with a large vortex occupying practically all the melt core and a vortex of lower intensity, which arises near the melt free surface during the lateral crystal growth and disappears at the cylindrical growth stage. To eliminate the second vortex, several hot zone modifications were analyzed. In Modification 2, one can see that the melt flow is more uniform. Moreover, the melt temperature gradient decreases and the flow becomes less intensive. It follows from the computations that the crystallization front moves at a high rate and the growth process is stabilized sooner than in Modification 1. Note that a higher gradient in the crystal is observed near the seed, bottleneck, and along the crystallization front but it is lower in Modification 2 than in Modification 1. It is clearly seen in Fig. 4 showing the 1D temperature gradient distribution along the crystallization front for both modifications.

The model was verified by using available experimental data. A good agreement between the computational and the experimental crystallization shapes (Fig. 1) indicates that the model provides an adequate prediction of the temperature fields in the reactor.

### 4. Conclusion

We have presented a numerical approach for the simulation of single leucosapphire crystal growth by the Kyropoulos method. This approach uses a minimal set of simplifications and estimates of the temperature at any point of the reactor, which is very difficult to do experimentally. In addition, the model accounts for the effects of the parameters and design of the reactor parts on the temperature fields. Moreover, the model can estimate the temperature gradient in the crystal and in the melt, the heat flux distribution depending on the materials of the reactor parts, geometry of the crystallization front, and the power consumption. The model has been tested using the industrial furnace designed by Monocrystal Inc. A good agreement between the computations and the data indicates an adequate prediction of the temperature fields in the reactor. With these findings of the global heat transfer, Monocrystal Inc. has

begun to design an experimental growth reactor with the modifications of the reactor parts to produce sapphire crystals of better quality. New engineering ideas can now be tested using numerical simulation before their experimental realization.

## 5. References

- [1] E.V. Yakovlev, V.V. Kalaev, I.Yu. Evstratov, Ch. Frank, M. Neubert, P. Rudolph, Yu.N. Makarov, Global heat and mass transfer in vapor pressure controlled Czochralski growth of GaAs crystals, *J.Crystal Growth*, 252/1-3 (2003) pp. 26-36
- [2] D.P. Lukanin, V.V.Kalaev, Yu.N. Makarov, T. Wetzel, J. Virbulis, and W. von Ammon, Advances in the simulation of heat transfer and prediction of the melt-crystal interface shape in silicon CZ growth, *J.Crystal Growth*, 266/1-3 (2004) pp. 20 - 27
- [3] V.M.Mamedov, S.A. Rukolaine, Numerical solution of problems with radiation transfer in axisymmetric areas of a complex shape with specular Fresnel's, *Math. Modeling*, vol. 16, №10 (2004) pp.15-28

## 6. Figures



Fig. 1. Sapphire boule with a diameter up to 300 mm and 65 kg weight, grown by *Monocrystal Inc.* in Stavropol (Russia) using the Kyropoulos technique (left) and the sapphire crystal photo at an intermediate growth stage (right).

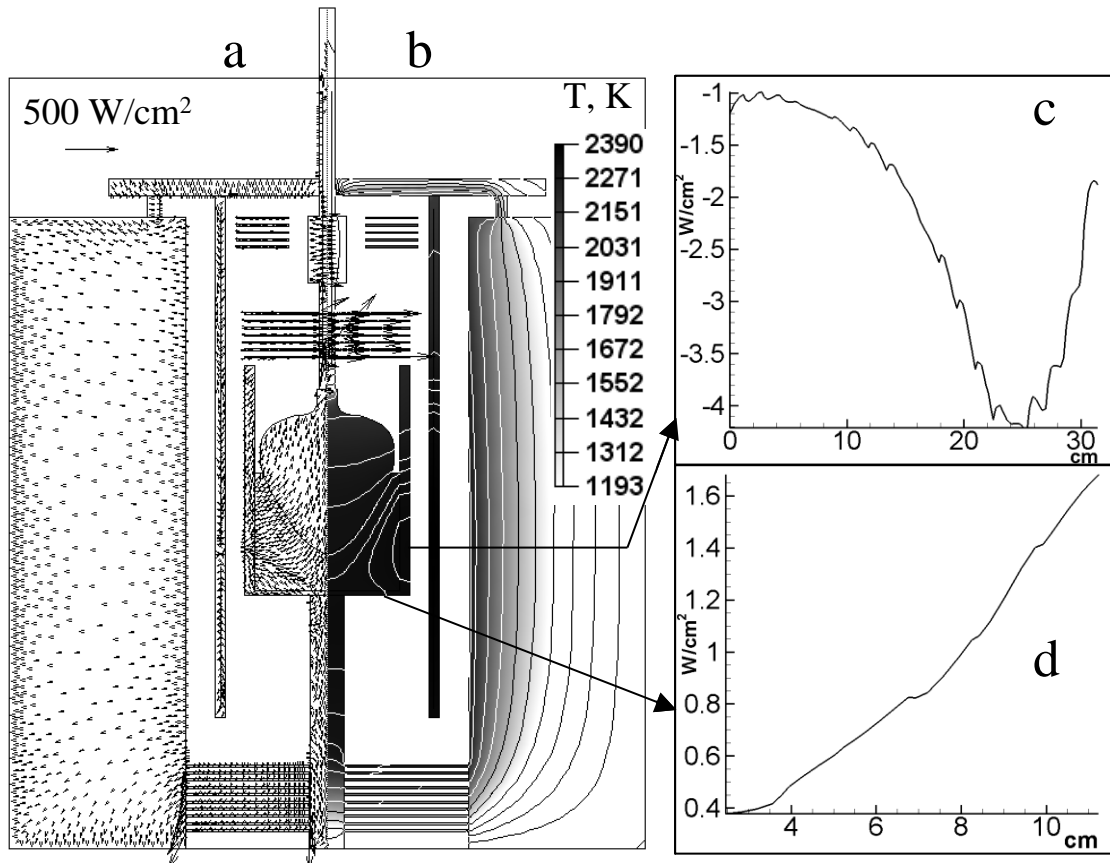


Fig. 2. The heat flux vector (a) and the temperature (b) distributions in the reactor and 1D distribution of the heat flux along the side wall (c) and the bottom (d) of the crucible.

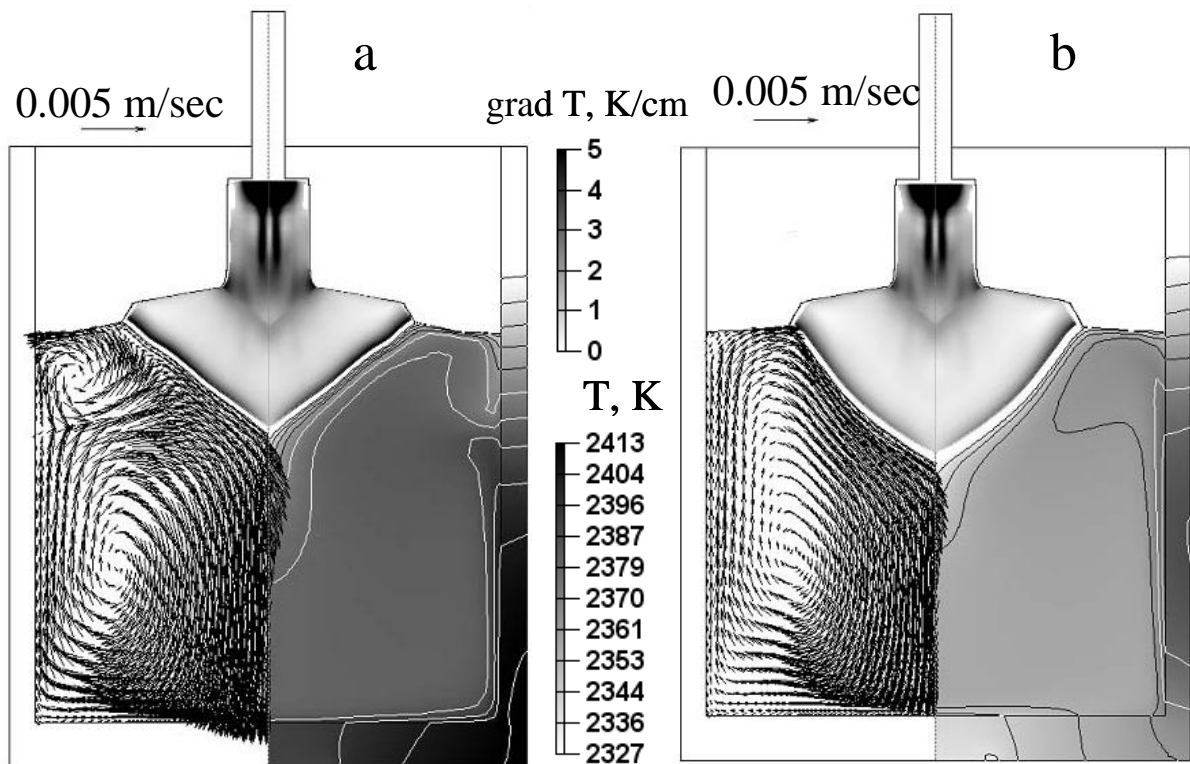


Fig. 3. The distributions of the temperature gradient in the crystal, the temperature in the melt and the crucible (on the right), and the flow pattern in the melt (on the left) in the industrial reactor for Modification 1 (a) and Modification 2 (b).

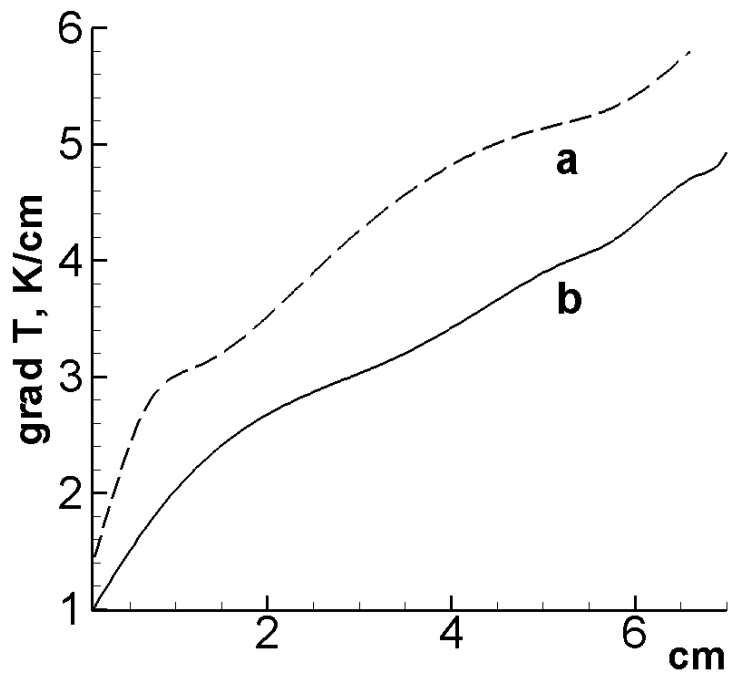


Fig. 4. The temperature gradient distribution along the crystallization front from the axis of symmetry to the periphery for Modification 1 (a) and Modification 2 (b).